Iodine distribution and volatilization in contrasting forms of forest humus during a laboratory incubation experiment

Marine Roulier, Loic Carasco, Isabelle Le Hécho, Maïté Bueno, Daniel Orjollet, Florence Pannier, Manuel Nicolas, Frédéric Coppin

Iodine distribution and volatilization in contrasting forms of forest humus during a laboratory incubation experiment

Abstract

Radionuclides ^{129}I ($t_{1/2}$ = 15.7×10^6 years) and ^{131}I ($t_{1/2}$ = 8.02 days) are both introduced into the environment as a result of nuclear human activities. Environmental transfer pathways and fluxes between and within ecosystems are essential information for risk assessment. In forest ecosystems, humus degradation over time could result in re-mobilization and then downward migration and/or volatilization of intercepted ^{129}I. In order to estimate the scale of these processes, humus (mull and moder forms) sampled under deciduous and coniferous forests were spiked with $^{125}I^-$ ($t_{1/2}$ = 59.4 days), as a surrogate for ^{129}I, in order to study the evolution of its water-soluble and organic fractions as well as the volatilization rate during humus degradation at laboratory scale. To our knowledge, this is the first time that interactions between iodine and contrasting forms of forest humus have been investigated. The evolution of native stable iodine (^{127}I) pools in unspiked humus was also studied.

The nature of the humus' organic matter appears to be a factor that impacts on the proportions of water-soluble and organic fractions of iodine and on their evolution. Iodine-125 was mainly organically bound (fraction for mulls and moders: ~54-59 and 41-49%, respectively) and no clear evolution was observed within the 4-month incubation period. A large decrease in ^{125}I water-solubility occurred, being more marked for mull (from ~14-32 to 3-7%) than for moder (from ~21-37 to 7-19%) humus. By contrast, a significant fraction was not extractible (~38-43%) and varied in inverse proportion to the water-soluble fraction, suggesting a stabilisation of iodine in humus after wet deposit. The nature of the humus organic matter also impacted on ^{125}I volatilization. Although of the same order of magnitude, the total volatilization of ^{125}I was higher for moders (~0.039-0.323%) than for mulls (~0.015-0.023%) within the 4-month incubation period. Volatilization rates for mulls were correlated with the water-soluble fraction, implying that volatilization of ^{125}I could occur from the humus solution. Our results

showed that humus is thus a zone of iodine accumulation by association with organic matter and that potential losses by lixiviation are significantly more important compared to volatilization.

Keywords: Iodine; solubility; volatilization; organic matter; forest

1. Introduction

Natural iodine (I) is composed of ^{127}I, its single stable isotope, and the long-lived radionuclide ^{129}I with a half-life of 15.7×10^6 years. Iodine-129 and iodine-131 ($t_{1/2}$ = 8.02 days) are both introduced into the environment as a result of nuclear human activities (e.g. atmospheric releases following nuclear accidents, reprocessing of radioactive wastes, and in the medical field). ^{131}I represents a significant and immediate health hazard associated with large-scale nuclear events (UNSCEAR, 2011); while ^{129}I, due to its extremely long half-life, is one of the most persistent anthropogenic radionuclides in ecosystems representing a challenge in terms of long-term management (Hou et al., 2009).

Among ecosystems liable to be affected by radioiodine atmospheric inputs, forests are of major interest because of their large and complex contact surfaces with the atmosphere. These ecosystems can be both a sink for elements via their interception and accumulation, and also a secondary source via their re-emission to the atmosphere and/or drainage to neighboring ecosystems (Ranger et al., 1995; Shaw, 2007). Our previous studies of the distribution of iodine in French forest soils have shown that humus could act as a temporary store of iodine from atmospheric deposition and litterfall, since the net iodine accumulation rates in humus could account for up to 82.3% of annual iodine input to the soil (Roulier et al., 2018, 2019). Because the humus layer is in a key position as a transition zone between the atmosphere and the soil, a better understanding of iodine behavior in this forest compartment would help improve

estimated fluxes through its interfaces, essential for relevant modelling of iodine dynamics in forests. Humus is made up of the organic matter part of the soil resulting from chemical and microbiological decomposition of vegetal deposits. This organic matter layer is composed of humic substances (i.e., fulvic and humic acids, humins) and macro-, meso- and micro-fauna. Mull humus form is subject to rapid degradation of litter linked to high biological activity, while moder and mor forms are characterized by a lower to almost nil biological activity, resulting in intermediate to extremely low turnover of organic matter, respectively (Baize et al., 2009).

Iodine occurs in several oxidation states in the environment as inorganic (iodide (I^-) and iodate (IO_3^-)) and organic species. Metal oxides and hydroxides (e.g. $Fe(OH)_3$, $Al(OH)_3$ and MnO_2) can play a role in iodine retention in soils due to the their amphoteric sites (Dai et al., 2004; Muramatsu et al., 1990; Shetaya et al., 2012; Whitehead, 1973, 1978). Although the link between iodine and soil organic matter (OM) has been reported in various studies (e.g. Bostock et al., 2003; Dai et al., 2009; Roulier et al., 2019; Santschi et al., 2017; Schwehr et al., 2009; Shimamoto et al., 2011; Steinberg et al., 2008a, 2008b; Whitehead, 1973; Xu et al., 2012), few studies have focused specifically on the humus compartment (Bostock et al., 2003; Söderlund et al., 2017; Takeda et al., 2015). Mechanisms governing the incorporation of inorganic iodine into organic matter have been the subject of several studies. Iodate and iodide have been shown to be reduced and oxidized, respectively, to reactive intermediate species (HIO and I_2) reacting with organic molecules possessing electron donating groups such as phenols (Franke et Kupsch, 2010; Fukui et al., 1996; Reiller et al., 2006; Schlegel et al., 2006; Warner et al., 2000; Whitehead, 1974). Additionally, Schlegel et al. (2006) showed that iodine was linked to aromatic rings in naturally iodinated humic substances. The iodination of amines through the formation of iodine–nitrogen bonds from amino groups in organic matter has also been demonstrated both in synthetic solutions (Franke and Kupsch, 2010) and in humic substances extracted from soil (Xu et al., 2013). Iodine in humus can be leached during rainy events, which

77 may affect its distribution in soils, groundwater, surface water and vegetation. Studies based on
78 chemical extractions to evaluate the importance of the water-soluble fraction of iodine in soils
79 have shown that it may be significant (up to 25% of total soil iodine) (e.g. Ashworth et al.,
80 2003; Bostock et al., 2003; Hansen et al., 2011; Hou et al., 2003; Johnson, 1980; Qiao et al.,
81 2012; Takeda et al., 2015). In addition, although organic matter could decrease the water-
82 solubility of soil iodine, its dissolved fraction may also be a source of dispersion of iodine due
83 to the formation of colloidal or dissolved organic material (Chang et al., 2014; Unno et al.,
84 2017; Xu et al., 2011a, b). The importance of the link between iodine and dissolved organic
85 matter has been reported by Xu et al. (2011a) explaining that a small and easily mobilized
86 fraction of OM could behave as a source of iodine under colloidal organic form.

87 Regarding iodine volatilization, data in the literature are available only for the soil
88 compartment. A fraction of iodine in soil can be volatilized as I_2 or CH_3I, following abiotic
89 and/or biotic processes (e.g. Allard et al., 2010; Keppler et al., 2003; Muramatsu and Yoshida,
90 1995). Sheppard et al. (1994) determined ^{125}I volatilization from peat soil in laboratory
91 experiments and found a loss of only 0.07% over 66 days after addition for a spiking of about
92 7 kBq g^{-1}. Similarly, Bostock et al. (2003) found a minor ^{125}I loss by volatilization (total loss
93 of 0.011% over 22 days for a spike of approximately 1 kBq g^{-1}) from forest soils, due to the
94 high retention of iodine by OM. Although the amounts of volatile iodine reported from
95 laboratory experiments appear low, Sive et al. (2007) identified forests as a terrestrial source of
96 methyl iodide (CH_3I) in the North Carolina atmosphere.

97 Considering the lack of information regarding iodine re-mobilization during humus
98 degradation and subsequent downward migration and/or volatilization, we conducted
99 laboratory incubation experiments with an ^{125}I tracer in an attempt to quantify these processes.
100 In this study, ^{125}I was chosen in place of ^{129}I to facilitate direct measurements using gamma
101 spectrometry, enabling us to work at very low concentration levels and quantify volatilization

rates. Although iodine exists in the environment in the form of iodide and iodate, additions of ^{125}I were conducted only using iodide form. Under well-controlled conditions and considering six humus samples from coniferous and deciduous forests including mull and moder forms, our aims were to: 1) examine the evolution over time of the distribution of the iodine tracer between water-soluble and organic fractions, 2) compare the tracer dynamics to those of naturally-occurring stable iodine, and 3) estimate the volatilization rate of the iodine tracer occurring in parallel with its re-distribution.

2. Materials and methods

2.1. Humus sampling

Six humus samples were taken from four deciduous (Oak: CHP40 and CHS35; Beech: HET25 and HET29) and two coniferous (Silver fir: SP25 and SP63) forests of the French RENECOFOR network (the National Network for the long-term Monitoring of Forest Ecosystem) managed by the ONF (the French National Forest Board) (http://www.onf.fr/renecofor). Different forest species were chosen because of the wide variety of plant debris that can be supplied to the soil impacting the nature of the humus OM. The localition of these six sampling sites is shown in Supplementary Information (SI) Figure S1. Humus samples were representative of two extreme levels of OM turnover (classification according to Brêthes and Ulrich (1997)), i.e. fast (eumull and mesomull) and slow (dysmoder and moder) turnover (Table 1).

Table 1. Sites descriptions for the six humus samples studied. t_{resDM} corresponds to dry mass residence time in humus.

Plot	Type of tree species	Dominant tree species	Type of humus	t_{resDM} (year)[1]	Level of OM turnover
CHP40	Deciduous	Oak	Eumull	1.1	Fast
CHS35	Deciduous	Oak	Dysmoder	16.8	Slow
HET25	Deciduous	Beech	Eumull	3.1	Fast

HET29	Deciduous	Beech	Dysmoder	16.8	Slow
SP25	Coniferous	Silver Fir	Mesomull	4.8	Fast
SP63	Coniferous	Silver Fir	Moder	12.5	Slow

[1]from Roulier et al. (2019)

Sampling was carried out from 2 to 20 October 2017. About 2 kg (wet mass) of humus, carefully separated by hand, were sampled (height of sampling corresponding to a few centimetres above the mineral soil) and kept in closed plastic bags. An additional sorting was performed in the laboratory to remove moss and branch debris, then humus were cut with a chisel (size of pieces: ~1cm) before measuring their field water content (calculated as the ratio of the weight of water to the weight of dry humus). Water content varied between 100 and 300%, close to that used by Cotrufo et al. (2010) to quantify litter decomposition rates. Samples were stored at 4°C before being spiked with iodide-125.

2.2 Set-up and monitoring of the incubation experiment

2.2.1. Preparation of humus samples: ^{125}I spiked and unspiked samples

The six humus samples were spiked with the radioisotope ^{125}I ($t_{1/2}$ = 59.9 days) in iodide (I^-) form. The spike solution was prepared by a 1000-fold dilution of certified solution (LEA, ORANO) with ultra-high quality (UHQ) water (Millipore, >18.2 MΩ·cm), giving a chemical composition of 15 pg g^{-1} (10 kBq) of ^{125}I, 50 ng g^{-1} of $Na_2S_2O_3$ and 50 ng g^{-1} of NaI. Between 152 and 181 g (dry weight, dw) of humus were placed in a plastic tray and contaminated uniformly with the spiking solution (approx. 40 kBq g^{-1} dw of ^{125}I (62 pg g^{-1})). To obtain a homogeneous contamination of the humus, these were saturated in solution (uniform addition of spiking solution volume until water saturation). The spiked humus samples were air-dried until the target water content of the humus was reached, with final water content of approx. 300-800% compared to dry humus weight. This was then mixed using a metal spatula. The homogeneity of the spiked humus was estimated by comparing expected theoretical activity

with actual activity measured. Two aliquots of each spiked humus samples were analysed using gamma spectrometry after drying at 40°C in an oven. This low drying temperature was used to prevent the volatilization of iodine at higher temperatures. The mean difference between expected activity and measured activity was 11 ± 9 %, which was close to the variability obtained between duplicates (10 ± 4 %) and the measurement uncertainty (≈ 10 %). After sampling for time zero (t-0) measurements (see §2.4.) and validating sample homogeneity, the six spiked humus samples were transferred into 2 L glass bottles, in duplicate (named samples R1 and R2 for each sample) using a metal spatula. The twelve incubation bottles were then placed in the incubation chamber and connected to the activated carbon traps (Figure 1; see §2.2.2.). The incubation bottles were periodically shaken by hand (~ once a week) to homogenize water content. Their weights were monitored and, when needed, additional UHQ water was added to keep the targeted initial water content constant (SI Figure S2).

Unspiked humus samples used to monitor the evolution of naturally present stable iodine were treated following the same procedure, using UHQ water to reach the targeted initial water content. Due to expected low volatilized iodine concentrations and the difficulty in extracting stable iodine from the activated carbon traps, stable iodine volatilization was not monitored. The humus samples were sampled for t-0 measurements and transferred into six incubation bottles of 1 L using a metal spatula. For each sampling time, duplicate samples were taken from each bottle (named samples R3 and R4). The incubation bottles were also periodically shaken and their weights were monitored and, when needed, additional UHQ water was added to keep the targeted initial water content constant (SI Figure S2).

2.2.2. Incubation design

Figure 1 illustrates the experimental incubation system. The 18 bottles containing spiked and unspiked humus were placed in incubation chambers kept at a temperature of 28°C to

optimise the humus decomposition rate (Pietikäinen et al., 2005). Each incubation bottle was connected to a CO_2-free air gas inlet that was calibrated at 20 ± 2 mL min^{-1}. Volatile ^{125}I produced within the incubation period was trapped at the system outlet on activated carbon (CHEMVIRON CARBON, nuclearcarb, grade 207B 1.5KI) traps conditioned in glass tubes (~7g per trap) with seal and glass wool. Two activated carbon traps were placed in series to ensure total trapping of volatile iodine.

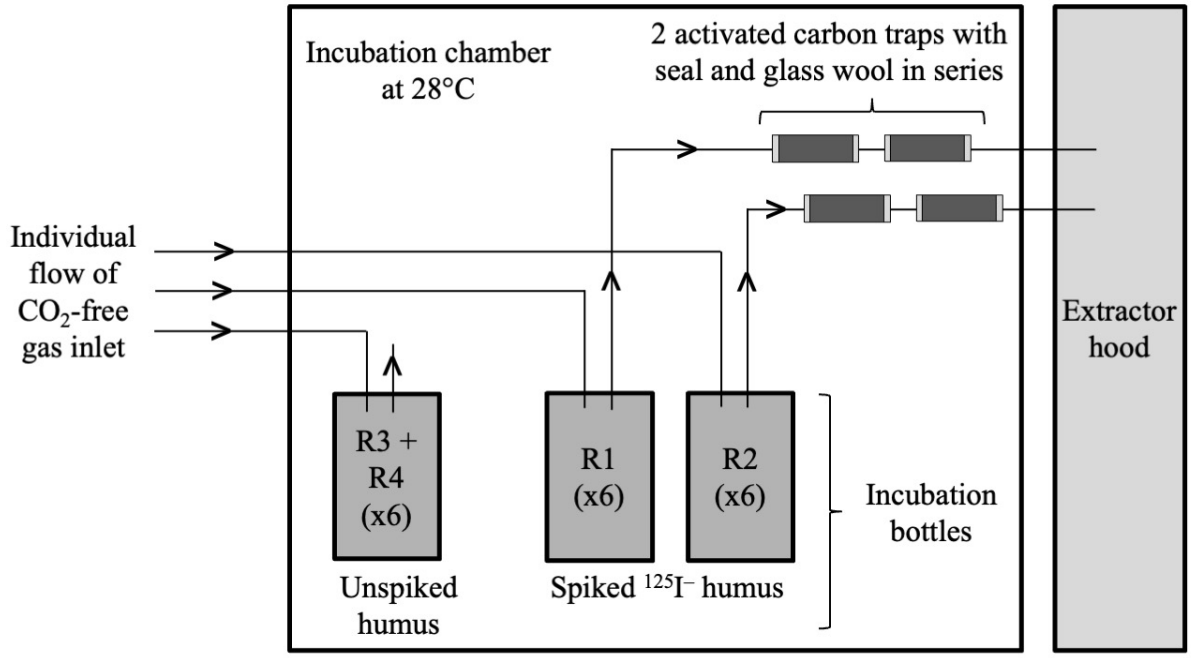

Figure 1. The experimental incubation system.

2.2.3. Humus and activated carbon traps sampling

The incubation bottles of spiked humus were periodically opened to sample about 5 g (dw) of humus for measurement (n = 1 per incubation bottle). About 2.5 g were dedicated to water content determination, and subsequent measurements of total ^{125}I activity and carbon-to-nitrogen (C/N) ratio after drying at 40°C were performed (see §2.4.). About 2 g (dw) were subjected to successive extractions with UHQ water and tetra methyl ammonium hydroxide (TMAH) (see §2.3.1.). About 0.5 g (dw) was used to determine total ^{125}I using the same protocol

used to determine ^{127}I in order to estimate extraction efficiency (see §2.3.2.). These samplings were performed six times after t=0, i.e. at 7, 14, 35, 56, 84 and 112 days of the incubation (referred to as t-0, t-7, t-14, t-35, t-56, t-84 and t-112, respectively).

Unspiked humus were sampled only at the end of incubation period to perform the same analyses (except for radiotracer activity). Sampling was performed in duplicate for each incubation bottle (R3 and R4).

During the incubation period, the active carbon traps were sampled at intervals of days at the beginning of incubation to weeks at the end of incubation. The activated carbon traps were transferred from the glass tube to a plastic tube for γ-spectrometry measurements (see §2.4.1). The ^{125}I volatilization rate (d^{-1}) was defined as the ratio of ^{125}I activity measured in the activated carbon traps during the sampling time (Bq d^{-1}) and total activity of ^{125}I in the incubation bottle (Bq).

2.3. Samples treatment for total and chemical extractions of iodine

2.3.1. Successive chemical extractions of humus iodine

A sequential extraction procedure was used to estimate pools of water-soluble iodine (i.e. w-soluble fraction) and iodine associated with OM (i.e. organic fraction) in humus (Hansen et al., 2011; Shetaya et al., 2012). At each sampling time, the target iodine pools were obtained after 1) three successive extractions with UHQ water (w-soluble fraction), followed by 2) three successive extractions with 5% TMAH (organic fraction) at room temperature, as previously optimised for soil samples (Roulier et al., 2018). Final ^{125}I and ^{127}I concentrations in the solid and solution obtained at each stage of the three successive extractions were plotted and fitted with a linear regression model to generate y-intercepts corresponding to the percentage of the considered available ^{125}I and ^{127}I fraction (Teramage et al., 2018). About 9-15 g of wet humus were weighed in a 50 mL polypropylene sterile centrifuge tube, then a given volume of

extracting solution (UHQ water or 5% TMAH, Sigma-Aldrich, Germany, 25 wt% in H_2O) was added (i) to keep wet humus in constant contact with the solution, and (ii) to maintain the same v/w ratio (dry weight) in successive extractions (volume ranged between 18 and 30 mL according to humus sample). For each extraction step, tubes were mechanically stirred at room temperature for 3 h at 300 rpm (IKA, KS250). After centrifugation at 10,000 g for 25 min (w-soluble fraction) or 40 min (organic fraction), supernatants were filtered (0.22 µm, PES filter) and stored at 4°C until analysis was performed. Reagent blanks were subjected to the same procedure. The residual fraction was calculated as the difference of total iodine in the humus minus the sum of w-soluble and organic fractions.

2.3.2. Total iodine extraction

Alkaline extraction using TMAH was performed to determine total ^{127}I in unspiked humus samples (Shetaya et al., 2012; Watts and Mitchell, 2008). Approximately 0.5 g dry mass of humus was weighed directly into a 50 mL DigiTUBE (polypropylene) and mixed with 10 mL of 5% TMAH. Reagent blanks were added in each digestion run. Tubes were placed at 90°C for 3h on a sand bath (t-0) or in a temperature-controlled digestion system (DigiPREP, SCP Science) (t-112). After heating, solutions were diluted to 20 mL using UHQ water. After settling overnight, digested samples were filtered at 0.22 µm (PES filter) and stored at 4°C until analysis by inductively coupled plasma mass spectrometry (ICP-MS) for ^{127}I (see §2.4.1). The same procedure was used for ^{125}I spiked humus in order to estimate extraction efficiency by comparing it with direct solid gamma spectrometry analysis. Extraction efficiency ranged from 70 to 85% and was used to calculate total ^{127}I concentrations in humus at t-0 and t-112.

2.4. Iodine, pH, carbon, nitrogen and microbial activity measurements

2.4.1. Radioiodine (^{125}I) and stable iodine (^{127}I)

The ^{125}I analysis for both liquid extracts and solid samples was carried out using a hyper pure germanium gamma spectrometer (Itech Instruments, GCD 30-190X). All activity measurements were decay-corrected back to 1 December 2017. The detection limit was around 0.3 Bq per sample (0.015 Bq mL^{-1} for a 20 mL sample) and analytical uncertainty was around 4% (1σ).

The stable iodine analysis was performed using an Agilent 7500ce ICP-MS (Agilent Technologies, Tokyo, Japan) using external calibration in UHQ water (water samples) or 0.05% TMAH (organic fraction and total iodine extraction). The instrument detection limits of iodine ranged between 0.07 and 0.89 µg L^{-1} depending on the sample matrix. Analytical uncertainty was <5% (relative standard deviation (RSD), 10 replicates).

2.4.2. pH, total carbon and nitrogen, and dissolved organic carbon

pH was measured in the first water extract (pH_{water}). The carbon and nitrogen contents of the solid samples were determined using a CHNS Elemental Analyzer (Elementar, Vario El cube). The quantity and quality of organic matter were determined using a microplate reader (TECAN M1000). UV-absorbance measurements (of the three extracts with UHQ water and TMAH) were used for organic carbon determination (Carter et al., 2012) and fluorescence measurements (for the first extract with UHQ water and TMAH) (λ_{ex}370 nm and λ_{em}450 and 500 nm) to calculate fluorescence index (FI) as the ratio of emission intensity at 450 nm to that at 500 nm for a fixed excitation wavelength of 370 nm (Johnson et al., 2011; McKnight et al., 2001). The FI is commonly employed as an indicator of dissolved organic carbon quality. McKnight et al. (2001) demonstrated that the FI decreased as a function of aromaticity for fulvic acid samples.

2.4.3. Microbial activity

As OM degradation (e.g., Pietikäinen et al., 2005) and iodine volatilization (i.e., Amachi, 2008; Muramatsu et al., 2004) can be due to microbial activity, community-level physiological profiles (CLPP) were assessed using the Biolog EcoPlate™ (Biolog, Hayward, CA, USA). These contain 31 of the most useful carbon sources (C-sources) for soil community analysis in triplicate and three controls with no substrate. The formation of purple colouring and an increase in optical density at 590 nm (OD_{590}) occur when microorganisms use the carbon source and begin to respire (Leflaive et al., 2005; Biolog data sheet). About 1 mL of the first water-extract (n = 1) was recovered prior to filtration and diluted 5-fold to give a w/v ratio of 1/100 (Pohlad and Owen, 2009) with 0.22 µm filtered UHQ water (PES). For each plate, 150 µL of water-extracts of two humus samples and one blank were inoculated into microplate wells and incubated at 25°C in the dark for up to 96 hours. The OD_{590} was measured every 24 hours for 4 days using a microplate reader set to a wavelength of 590 nm (TECAN M1000). The OD_{590} measured was corrected by subtracting the value of the respective control well (net OD_{590}). Negative values that occasionally resulted were set to zero. The final reading time was chosen by counting the number of wells at time point (n_t) for which net OD_{590} exceeds 0.1. The time with the greatest change (i.e. $n_t - n_{t-1}$ was maximum) was selected (Glimm et al., 1997; Grove et al., 2004). After counting for overall plates and communities, the reading time of 48 h was thus selected. In order to evaluate changes in CLPP over incubation time and among different forms of humus, the number of positive C-sources, i.e. with a net OD_{590} above of 0.4, was enumerated (Colinon-Dupuich et al., 2011; Verschuere et al., 1997). The substrates were also assigned to guilds according to their chemical nature (Choi and Dobbs, 1999; SI Table S1). Following the procedure described by Leflaive et al. (2005), guilds were equally weighted to the largest one (carbohydrates, 10 substrates) from Eq. 1 for the guild x with *n* substrates:

$$S_x = \frac{10}{n} \times \sum_{i=1}^{n} \text{net } OD_{590}\ (substrate\ i) \quad \text{(Eq. 1)}$$

To factor in differences in guild size, the calculated value S_x was divided by their sum resulting in the new value P_x (Eq. 2):

$$P_x = \frac{S_x}{\sum_{i=1}^{6} S_i} \quad \text{(Eq. 2)}$$

2.5. Modelling the kinetic evolution of iodine pools

The evolutions of ^{125}I w-soluble, organic and residual fractions over time were modelled according to a first kinetic law in the following form (Eq. 3):

$$y = (A_0 - A_f) \times e^{-kt} + A_f \quad \text{(Eq. 3)}$$

Where A_0 = percentage of the ^{125}I-pool considered at t-0; A_f = final percentage of the ^{125}I-pool considered once stabilization is reached; k = rate coefficient (day^{-1}); t = incubation time (day).

In line with Bostock et al. (2003) and their modelling of iodine volatilization rates over time using a first kinetic law, the cumulative fluxes of volatilized ^{125}I were modelled with using first kinetic law in the following form (Eq. 4):

$$A_t^v = A_f^v \times (1 - e^{-k_v t}) \quad \text{(Eq. 4)}$$

Where A_f^v = cumulative volatilized ^{125}I at time t (mol); A_f^v = maximum cumulative of volatilized ^{125}I (mol); k_v = rate coefficient (day^{-1}); t = incubation time (day).

Equations 3 and 4 were solved by the least square method, fitting the model to the data observed in this study.

3. Results

3.1. Evolution of humus parameters during incubation

Mean values of pH_{water}, carbon content (%C) and the carbon-to-nitrogen (C/N) ratio of humus during the incubation period are presented in Table 2. Values for each sampling time are presented in SI Table S2 and Table S3.

Table 2. Mean values (± standard error) of pH_{water}, carbon content (%C) and carbon-to-nitrogen (C/N) ratio of spiked (R1 and R2) and unspiked (R3 and R4) humus.

		pH_{water}	**%C**	**C/N ratio**
CHP40 (mull)	R1-R2	6.4 ± 0.3	41.1 ± 1.6	19.4 ± 1.6
	R3-R4	6.3 ± 0.2	39.5 ± 2.4	20.6 ± 1.9
CHS35 (moder)	R1-R2	6.1 ± 0.9	42.7 ± 1.1	16.4 ± 1.1
	R3-R4	6.4 ± 0.5	42.7 ± 0.6	17.7 ± 0.6
HET25 (mull)	R1-R2	6.9 ± 0.4	35.5 ± 1.6	20.0 ± 1.1
	R3-R4	6.4 ± 0.5	32.9 ± 1.3	19.2 ± 0.9
HET29 (moder)	R1-R2	6.2 ± 0.3	44.4 ± 1.6	18.6 ± 1.6
	R3-R4	6.1 ± 0.3	44.1 ± 0.9	20.0 ± 1.8
SP25 (mull)	R1-R2	7.2 ± 0.4	39.3 ± 1.9	24.2 ± 2.5
	R3-R4	6.9 ± 0.4	38.7 ± 2.0	25.7 ± 1.2
SP63 (moder)	R1-R2	5.8 ± 0.5	46.1 ± 1.2	20.7 ± 1.5
	R3-R4	5.4 ± 0.4	45.0 ± 0.6	21.3 ± 0.8

On average over the incubation time, pH_{water} showed no significant variation. CHP40, CHS35, HET29 and SP63 humus were slightly more acidic (pH_{water} ~5-6) than HET25 and SP25 humus (pH_{water} ~7). The carbon content showed no significant variation during incubation and ranged from 33 to 46% depending on the humus sample. The C/N ratios were ~19-26 for mull forms (i.e. CHP40, HET25 and SP25) and ~16-21 for moder forms (i.e. CHS35, SP63 and HET29), and remained relatively constant across the incubation period. According to Duchaufour (1950), OM with a high C/N ratio (~15-20) decomposes slowly, and results solely in the release of carbon dioxide, with total nitrogen being used for microbial syntheses. For the first water-extract (W1), concentrations of dissolved organic carbon (DOC) were higher for moder than for mull humus (SI Table S4 and Table S5; on average, ~360-540 and ~150-340 mg L^{-1} for spiked humus; ~215-300 and ~ 70-210 mg L^{-1} for unspiked humus, respectively), probably due to slightly higher carbon content (~43-46 and 36-41%, respectively; Table 2). The fluorescence index (FI) in TMAH-extracts was usually lower than in water-extracts, suggesting that, as expected, TMAH-extracted organic matter was more aromatic than that solubilized in water (SI Figure S3; McKnight et al., 2001). Moreover, FI values showed no clear significant evolution over the incubation period. As detailed analysis regarding the composition of residual

humus was not carried out, the nature of the molecules constituting the residual fraction is unclear. However, it can be expected that the residual fraction would be composed of more complex OM and, therefore, remains undissolved in both water and TMAH. The aromaticity or molecular weight of the OM could increase depending on the strength of the extractant: w-soluble < TMAH-available < residual fractions.

Community-level physiological profiles (CLPP) assessed with the Biolog EcoPlate™ for spiked humus are presented Figure 2 (a). At t-0, the number of positive C-sources presented no clear difference between types of humus and accounted for ~70-90% of the sources tested. However, for CHP40, HET25 and SP25, the number of positive C-sources started to decrease at t-35 up to t-56 (~20-40% positive C-sources); whereas the number of positive C-sources slightly decreased up to t-56 (~50-60% positive C-sources) for HET29 and SP63, and remained constant for CHS35. Hence, in our incubation experiment, microbial activity in mull humus (i.e. CHP40, HET25 and SP25) decreased more rapidly that in moder humus (i.e. CHS35, HET29 and SP63). Regarding the chemical nature of the substrates (Figure 2 (b)), at t-0 the six spiked humus samples used the six guilds of C-source in almost the same proportions. However, in addition to a decrease in total bacterial activity at t-56, the substrates utilization was different compared to t-0. Bacteria in the CHP40 and SP25 humus used only 3-4 carbon guilds, and five carbon guilds in HET25 and CHS35. For HET29 and SP63, the six guilds of C-source were used throughout the experiments in varying proportions during incubation. No difference in substrate use depending on their chemical nature was found according to humus form.

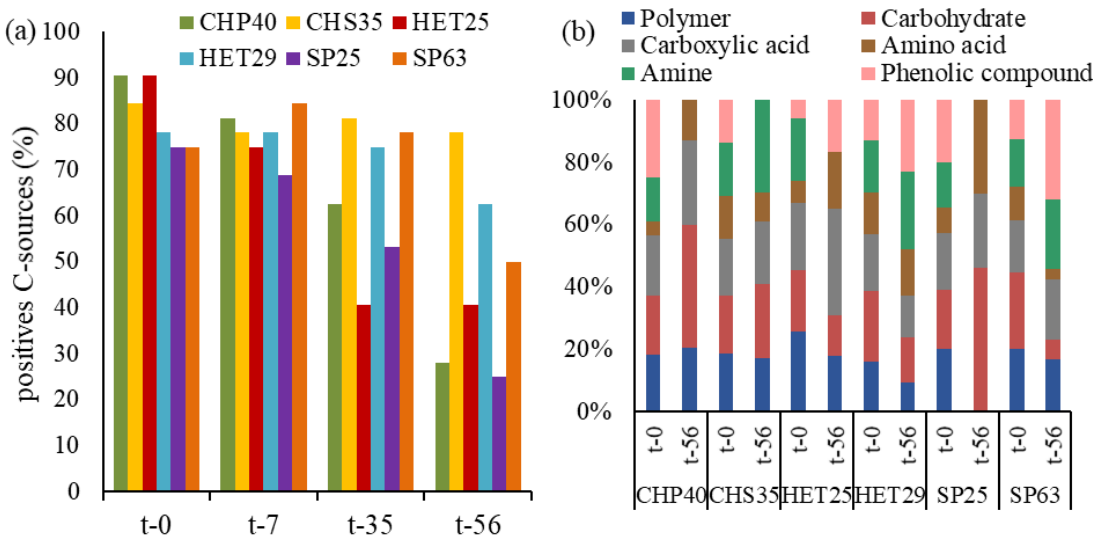

Figure 2. (a) Proportion of Biolog EcoPlate™ carbon sources accounted as positives for sampling time from t-0 to t-56, and (b) contribution of substrate guilds in total bacteria activity at t-0 and t-56 for spiked humus (R1, n = 1).

3.2. Evolution of iodine w-solubility and its organic-pool

The evolutions of w-soluble, organic and residual ^{125}I fractions are shown in Figure 3. The corresponding modelling results obtained from Eq. 3 (see §2.5.) are compiled in SI Table S6. Native w-soluble, organic and residual ^{127}I fractions at t-0 and at the end of experiment (t-112) for unspiked humus are compared to those of added ^{125}I in Figure 4. The corresponding detailed data are reported in SI Table S7 and Table S8 for spiked and unspiked humus, respectively.

Factoring in uncertainties, total ^{125}I activities were similar across the incubation period for all forms of humus, with a mean for duplicates and the seven sampling dates of: CHP40 = 37 ± 2, CHS35 = 42 ± 3, HET25 = 38 ± 2, HET29 = 42 ± 2, SP25 = 37 ± 2 and SP63 = 36 ± 2 kBq g^{-1} (SI Figure S4). Total concentrations of stable iodine naturally present in unspiked humus were constant over the incubation period for all forms of humus, ranging from 2.7 to 5.3 mg kg^{-1} with a mean for duplicates and the two sampling periods of: CHP40 = 2.7 ± 0.2, CHS35 = 3.5 ± 0.2, HET25 = 3.1 ± 0.2, HET29 = 5.3 ± 0.3, SP25 = 2.9 ± 0.7 and SP63 = 4.7 ± 0.3 mg kg^{-1}.

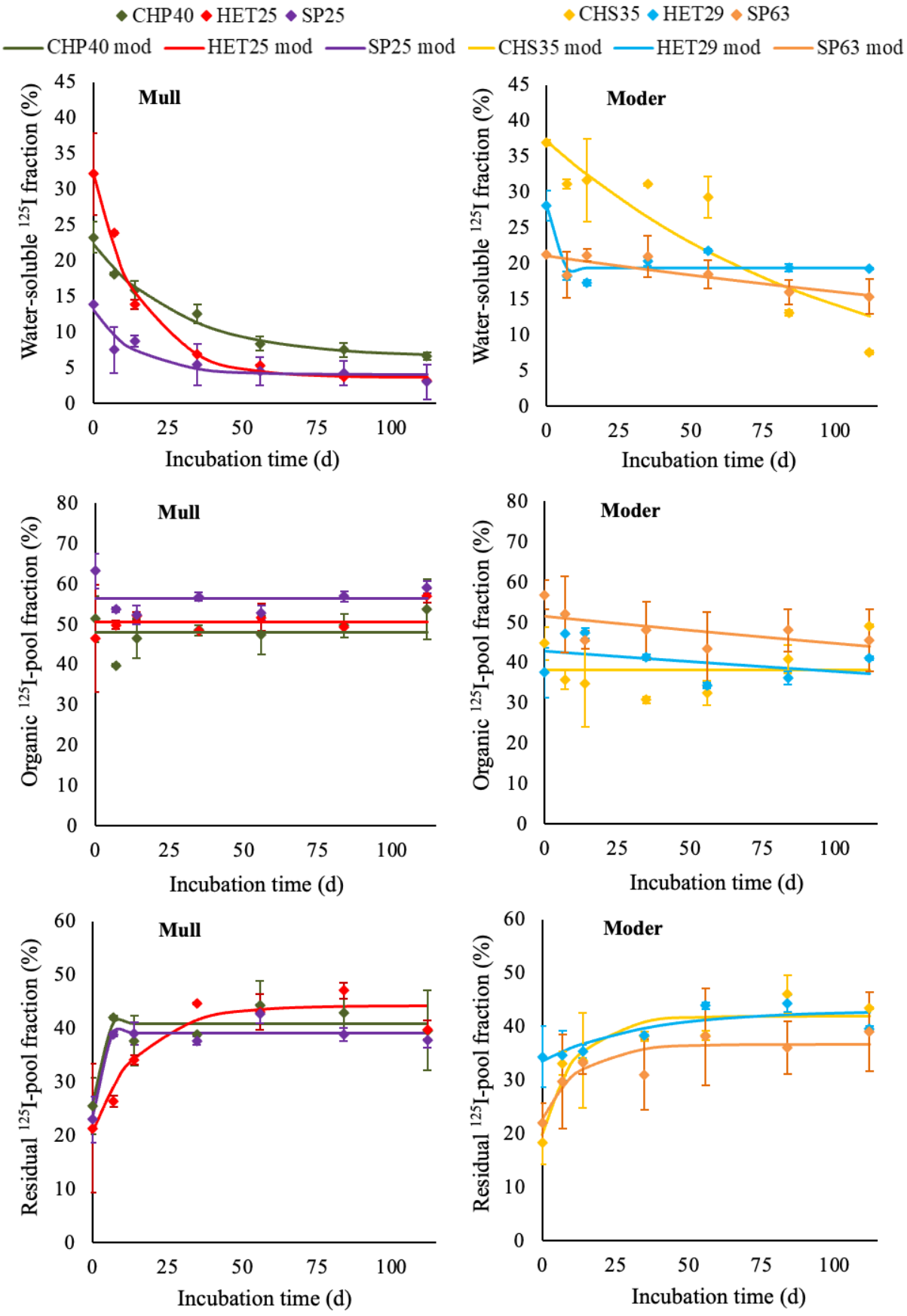

374

375 Figure 3. Evolution of w-soluble, organic and residual fractions of added ^{125}I according to
376 incubation time for mull and moder humus. Dots correspond to experimental mean of

duplicates (R1 and R2) with the standard error and lines correspond to the model fitted to experimental data.

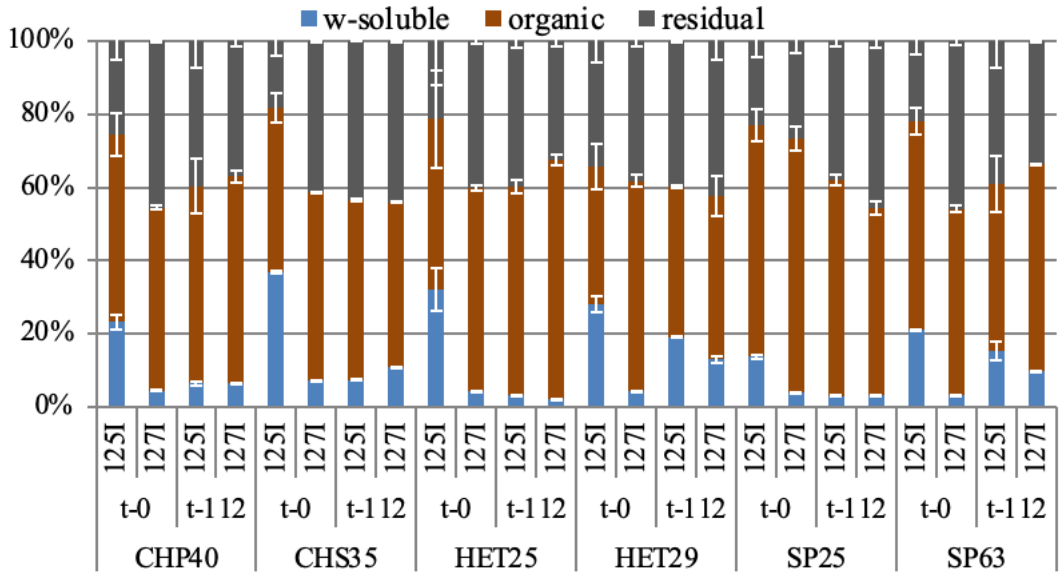

Figure 4. Native w-soluble, organic and residual ^{127}I fractions at the beginning (t-0) and at the end (t-112) of experiment for unspiked humus (R3 and R4), compared to those of added ^{125}I for spiked humus (R1 and R2). Mean values for duplicates and the standard error.

Significant differences in ^{125}I water-solubility were found between the humus samples with initial (t-0) proportions ranging from ~14 to 37% (CHS35 = 36.9 ± 0.4, HET25 = 32.1 ± 5.8, HET29 = 28.1 ± 2.1, CHP40 = 23.2 ± 2.2, SP63 = 21.2 ± 0.1 and SP25 = 13.8 ± 0.5%). A significant decrease in ^{125}I water-solubility occurred over the incubation time for all samples with different kinetics to reach at t-112: CHS35 = 7.5 ± 0.3, HET25 = 3.2 ± 0.1, HET29 = 19.2 ± 0.1, CHP40 = 6.6 ± 0.6, SP63 = 15.4 ± 2.4 and SP25 = 3.0 ± 0.1% (Figure 3). For mull humus samples, i.e. CHP40, HET25 and SP25, the w-soluble ^{125}I fraction decreased within the first 2-3 months of incubation by a factor of 3.5, 10.0 and 4.6, respectively, with kinetic constants varying by a factor of 2 (k_w ~ 0.034, 0.063 and 0.069 d^{-1}, respectively; $R^2 > 0.90$) and then remaining quite stable, to reach the lowest values measured. For moder humus, the shape of the decrease is different to that for mull humus. For HET29 humus, the initial proportion of w-soluble ^{125}I (~28%) decreased rapidly (< one week after contamination), and then stabilized with the highest proportion of w-soluble ^{125}I (~19%) at the end of incubation of all the humus

samples. CHS35 and SP63 humus presented a continuous and slowest decrease of their w-soluble ^{125}I fraction (k_w ~ 0.010 and 0.003 d^{-1}, respectively; $R^2 > 0.73$) from the beginning to the end of the study. Last, at t-112, ^{125}I was less w-soluble in moder humus compared to mull humus. Regarding the dry mass residence time in humus of 1.1-4.8 and 12.5-16.8 years for mull and moders, respectively (Table 1), the w-soluble ^{125}I fraction decreased 18-177 times faster than the degradation of humus (SI Table S6; $t_{1/2}$ = 10-20 and 72-258 days for mull and moder). These results suggest that rain controls the vertical migration of iodine by leaching in the first months following iodine deposition; while over a longer term, iodine migration is controlled by OM degradation. In the case of stable iodine, the w-soluble ^{127}I fraction was very low compared to the values obtained for ^{125}I at the beginning of the experiments (by factors of from 3 to 7) and evolved very little from t-0 to t-112 (factor ≈ 1.5) except for HET 29 and SP63 moder humus, in which the w-soluble ^{127}I fraction increased by a factor 3, while for HET25 mull humus, it was reduced by half (SI Table S8). At the end of the incubation period, w-soluble ^{127}I fractions in unspiked humus accounted for: CHP40 = 6.64 ± 0.01, CHS35 = 11.04 ± 0.06, HET25 = 2.21 ± 0.01, HET29 = 13 ± 1, SP25 = 3.32 ± 0.03 and SP63 = 9.72 ± 0.02%. After 4 months, w-soluble proportions of added ^{125}I were relatively similar to the results obtained for natural ^{127}I (Figure 4), implying that added ^{125}I and native iodine tended towards the same distribution. Furthermore, the nature of the humus appears to be a factor influencing the level of ^{125}I water-solubility and its evolution over time. Indeed, a rapid and large decrease in ^{125}I solubility occurred for mull humus (i.e. CHP40, HET25 and SP25), with the w-soluble fraction decreasing from ~14-32 to 3-7%; whereas for moder humus (i.e. CHS35, HET29 and SP63), the decrease in ^{125}I solubility was slower and smaller (from ~21-37 to 7-19%) (Figure 3). To our knowledge, this is the first study of iodine-humus interaction, so direct comparison with data in the literature is therefore difficult. However, our results obtained regarding the evolution of iodine w-solubility and its proportion at the end of incubation for humus agree with results

previously obtained for soil (Ashworth et al., 2003; Bostock et al., 2003; Hansen et al., 2011; Hou et al., 2003; Qiao et al., 2012; Takeda et al., 2015). All these authors, regardless of the type of iodine addition (stable or radioactive, iodide or iodate) in soil, observed a decrease in its w-soluble fraction over time. More precisely, for forest soils, Bostock et al. (2003) and Takeda et al. (2015) quantified a decrease in w-soluble spiked iodine fraction from > 50% to < 7% after around one month of incubation, which they attributed to rapid conversion of added inorganic iodine to insoluble organic iodine.

The TMAH-extraction showed that a high ^{125}I fraction was immediately associated with the organic pool with initial proportions of: CHP40 = 51 ± 6, CHS35 = 45 ± 4, HET25 = 46 ± 13, HET29 = 37 ± 6, SP25 = 63 ± 4 and SP63 = 57 ± 4% (Figure 3). Surprisingly, factoring in uncertainties, the proportions of organic ^{125}I did not change clearly during incubation, except in case of CHS35. For this humus, the organic ^{125}I fraction decreased to 31% up to t-35 and then increased to ~49% up to t-112. Mull humus (i.e. CHP40, HET25 and SP25) presented slightly higher organic ^{125}I fractions than moder humus (i.e. CHS35, HET29 and SP63): on average ~57 and 45% at t-112, respectively (Figure 3). For native iodine in unspiked humus, organic ^{127}I fractions evolved only slightly from t-0 to t-112 (a factor of 1.1-1.4; SI Table S8), and at the end of incubation that fraction accounted for an average of ~ 58 and 49% for mull and moder humus, respectively. Iodine-127 was therefore mostly organically bound in most samples (~45-65%) and, as observed for the w-soluble fraction, proportions of added ^{125}I measured in the organic fraction were close to native iodine distribution at the end of incubation (Figure 4). Similarly, Hansen et al. (2011) found that humic substances extracted with 5% TMAH contained about 49-60% of total ^{127}I and ^{129}I for a composite of Danish soils. In Qiao et al. (2012), ^{129}I and ^{127}I were mainly distributed in the OM-related fraction (38 and 55%, respectively). Ashworth et al. (2003) found that NaOH extracted on average 60% of added ^{125}I in soil. In Bostock et al. (2003), $^{125}I^-$ has been shown to associate mostly with humic substances

within the soil with 87% of added iodine extracted by NaOH. However, these authors indicated that this percentage was overestimated because the w-soluble ^{125}I fraction was included in this fraction, which is in line with our results. Xu et al. (2011b) demonstrated that humic substances accounted for around 55 and 46% of the total ^{127}I and ^{129}I in soils, respectively.

In our study, the initial proportions of residual ^{125}I-pool were relatively similar regardless of humus type (~19-26%), except for HET29 showing a slightly higher proportion (CHP40 = 25 ± 5, CHS35 = 18 ± 4, HET25 = 21 ± 12, HET29 = 34 ± 6, SP25 = 23 ± 4 and SP63 = 22 ± 4%; Figure 3). The proportions of residual ^{125}I increased within the first month of incubation with different kinetics to reach at t-112: CHP40 = 40 ± 7, CHS35 = 43.4 ± 0.2, HET25 = 40 ± 2, HET29 = 39.7 ± 0.4, SP25 = 38 ± 1 and SP63 = 39 ± 7%. The humus CHP40 and SP25 presented the fastest increase (for CHP40, stabilization after one week; for SP25, k_r ~ 0.56 d^{-1}; R^2 = 0.93) with initial proportion of residual ^{125}I multiplied by a factor of ~1.5 after only 14 days and remaining constant throughout the rest of incubation period. For the CHS35, HET25 and SP63 humus, initial proportions increased by a factor of ~2 to reach steady values after < two months (k_r ~ 0.09, 0.06 and 0.08 d^{-1}; R^2 = 0.89, 0.91 and 0.84; respectively). Last, the HET29 humus, whose initial residual fraction was the highest, presented the slowest and smallest increase (k_r ~ 0.03 d^{-1}, R^2 = 0.74). A relatively large part of ^{125}I (~40%) was therefore found in the residue not available with TMAH or UHQ water at room temperature. The same observation was made for native iodine in unspiked humus with residual proportion in the same order of magnitude (~33-46%) (Figure 4). Overall, the same evolution of ^{125}I was observed for all types of humus, with faster stabilization for CHP40 and SP25 and less amplitude and weaker stabilization for HET29 (Figure 3).

3.3. ^{125}I volatilization from humus

86 ± 21% of total volatilized ^{125}I was trapped in the first activated carbon trap, whereas only 14 ± 21% was trapped in the second trap. The evolution of ^{125}I volatilization rates over the humus incubation period is shown in SI Figure S5. Volatilization rates varied over the 125 days of monitoring, with extreme values ranging within three orders of magnitude (CHP40 = $5.7\times10^{-8} – 1.6\times10^{-5}$, CHS35 = $2.6\times10^{-8} – 1.3\times10^{-5}$, HET25 = $3.6\times10^{-8} – 0.4\times10^{-5}$, HET29 = $7.0\times10^{-8} – 1.5\times10^{-5}$, SP25 = $0.3\times10^{-8} – 0.9\times10^{-5}$, SP63 = $6.4\times10^{-8} – 8.7\times10^{-5}$ day^{-1}). Generally, initial ^{125}I volatilization rates declined over the experiment time, except in the case of SP63. This humus differed from the others since the ^{125}I volatilization rate increased over the first month, while no specific trend was seen in the following months. Moreover, ^{125}I volatilization rates from SP63 humus were higher than those for the other humus samples (by a factor of from 6 to 35), if maximum values are compared. The mean ^{125}I volatilization rates, estimated by the modelling of the cumulative fluxes of volatilized ^{125}I using Eq. 4 (SI Table S9; see §2.5.), were: CHP40 = $1.8 \pm 0.3 \times10^{-6}$, CHS35 = $3.0 \pm 0.4 \times10^{-6}$, HET25 = $1.2 \pm 0.2 \times10^{-6}$, HET29 = $3.8 \pm 0.3 \times10^{-6}$, SP25 = $1.4 \pm 0.3 \times10^{-6}$, SP63 = $26 \pm 10 \times10^{-6}$ day^{-1}, confirming that volatilization from the SP63 humus was the highest. Regarding cumulative iodine fluxes, a significant increase could be observed during the first two months of incubation, followed by lesser augmentation for all spiked samples, except for SP63 whose cumulative fluxes increased linearly with time (Figure 5). Although in the same order of magnitude, differences in total volatilized ^{125}I over the incubation periods were observed according to humus type. The total amount of volatile iodine appeared slightly higher for moder humus (0.039 ± 0.004, 0.045 ± 0.002 and 0.32 ± 0.14% for CHS35, HET29 and SP63, respectively) than for mull humus (0.023 ± 0.004, 0.015 ± 0.002 and 0.017 ± 0.003% for CHP40, HET25 and SP25, respectively). These amounts were relatively similar between duplicates (RSD = 5-26%), except in the case of SP63 (RSD = 62%). For all types of humus studied, ^{125}I volatilization rates were within the range of emission rates found in the literature for soils (Bostock et al., 2003; Muramatsu and Yoshida,

1995; Wildung et al., 1985). In Bostock et al. (2003), over 22 days incubation, ^{125}I volatilization rates from forest soil ranged between 6×10^{-7} and 5×10^{-5} day^{-1}, and initially declined steeply followed by a subsequent slower decline. After adding ^{129}I to soil, Wildung et al. (1985) found an averaged volatilization rate of 2×10^{-5} day^{-1} from soil over 14 days. Muramatsu and Yoshida (1995) found a rate of volatilization ranging between 0.4×10^{-5} to 4×10^{-5} day^{-1} over 80 days after adding $^{129}I^{-}$ addition onto unplanted non-flooded soil.

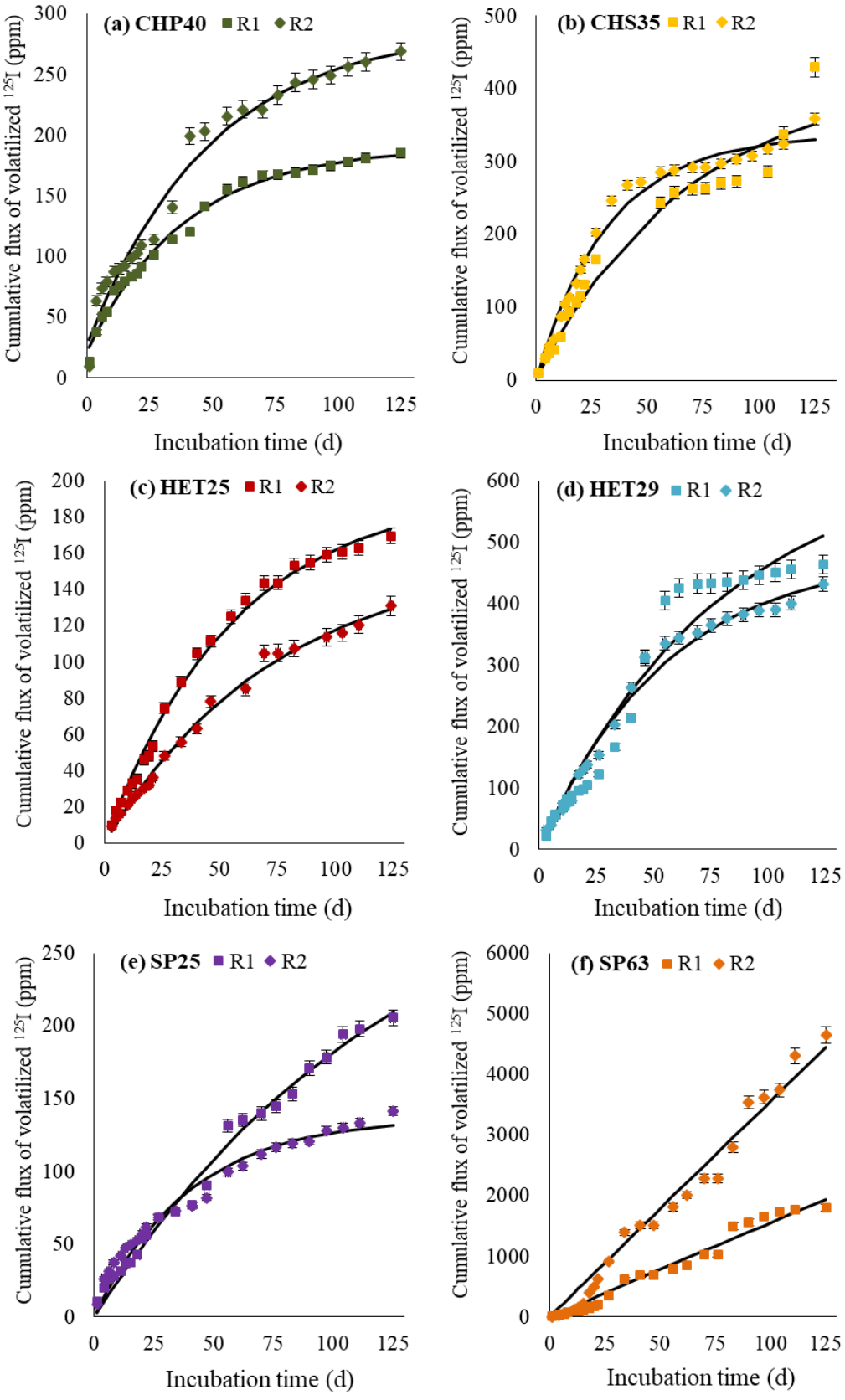

Figure 5. Cumulative flux of volatilized ^{125}I over the 125 days monitoring period for each humus (mull: (a) (c) (e), moder: (b) (d) (f)). R1 and R2 correspond to duplicates. Dots correspond to experimental values with standard deviation and lines correspond to model fitted to experimental data.

4. Discussion

Results from the current study suggest that humus is a zone of iodine accumulation by association with OM (organic and residual ^{125}I fractions = 37-63 and 38-43%, respectively) and that potential ^{125}I losses by lixiviation are far more significant than those by volatilization (w-soluble and volatilized ^{125}I fractions = 3-19% and 0.01-0.47%, respectively).

It appeared that added ^{125}I was progressively more strongly linked to humus components, depleting the w-solubility of iodine and resulting in a distribution similar to that of native iodine at the end of incubation (Figure 4). This iodination seemed to evolve differently according to humus form. Indeed, the composition of moder humus, which probably contains more complex organic molecules (slow degradation) than mulls (fast degradation) would lead to slower iodination of complex organic molecules and therefore higher w-solubility of ^{125}I in moders than mulls (Figure 3). This would be consistent with previous studies showing that lowest molecular weight (LMW) humic substances react more easily with iodine due to greater surface area which may provide greater accessibility to reactive sites, unlike high molecular weight (HMW) humic substances, whose iodination could be time-dependent (Bowley et al., 2016; Xu et al., 2011a, 2011b). Moreover, in our study, moder humus showed a slight increase in the w-soluble ^{127}I fraction (Figure 4) suggesting a deiodination process and thus a weaker affinity of iodine with moder than mull humus, which is consistent with a weaker stabilization of the w-soluble ^{125}I fraction for HET29 and SP63 (Figure 3). Furthermore, ^{125}I and ^{127}I w-soluble concentrations were positively correlated with DOC concentrations in water-extracts (Figure 6), which were higher for moders than mulls (SI Table S4 and Table S5) leading to increased quantities of w-soluble ^{125}I and ^{127}I linked to dissolved OM. After water extraction of soils from the Savannah River site contaminated by ^{129}I, Xu et al. (2011b) indicated that some colloidal and dissolved organic matter was either iodinated by radioiodine in soil solution or co-released from solids containing radioiodine previously incorporated into the soil. During

batch sorption experiments of iodine in humus, Söderlund et al. (2017) also found an unidentified iodine species in the liquid phase analyzed using HPLC-ICP-MS, thus supporting the hypothesis of OM-I association in solution. More recently, Takeda et al. (2019) showed that the concentration of dissolved organic iodine, obtained by subtracting the I^- and IO_3^- concentrations from the total I concentration, was positively correlated with the DOC of the soil solution extracted by centrifugation from Japanese forest soils. Likewise, Xu et al. (2011a) showed that w-soluble ^{129}I in soil was mostly associated with a low molecular weight organic carrier (13.5–15 kDa). Hence, our results would indicate a dual role played by organic matter: (1) humic substances of HMW limiting DOC would be iodine sinks and (2) humic substances of LMW contributing to DOC would be a source for subsurface iodine dispersion, as previously observed by Chang et al. (2014) and Unno et al. (2017).

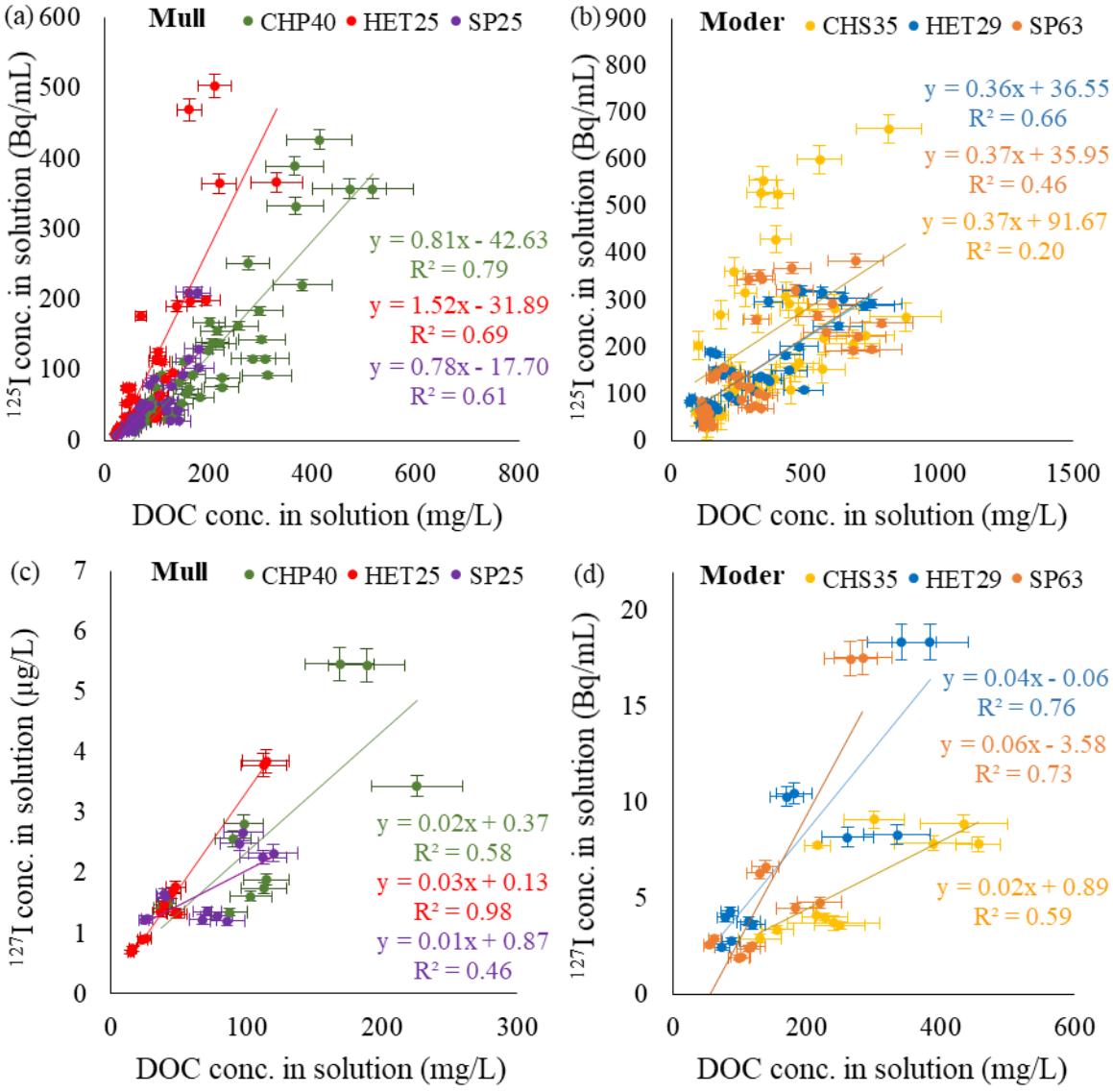

Figure 6. ^{125}I and ^{127}I concentrations in w-soluble extracts as a function of concentrations of dissolved organic carbon for the w-soluble fraction in mull and moder humus. Values (± standard error) for the duplicates and all sampling points.

Bostock et al. (2003) suggested that iodine association with OM occurred as a two-stage process according to their ^{125}I emission rates declining over time, initially rapid and then much slower. In the current study, the iodination process results in a reduction of the w-soluble iodine pool which might induce an effective reduction of the volatilization. This assumption is supported by the positive correlation between ^{125}I volatilization rate and w-soluble fraction for mulls (i.e. CHP40, HET25 and SP25; Figure 7 (a)(c)(e), $R^2 > 0.56$). However, no correlation

555 was found for moders (i.e. CHS35, HET29 and SP63; Figure 7 (b)(d)(f)), involving another
556 source of ^{125}I volatilization for this humus form in place of or additionally to the quantity of
557 iodine soluble in solution. As previously shown, the values for total volatilized ^{125}I activity were
558 higher for moder (~0.039-0.323%) than for mull (0.015-0.023%) humus, suggesting that ^{125}I
559 volatilization could occur directly from the solid phase of humus after its iodination. Iodide
560 could have been oxidised to reactive I_2 by reaction with hydroquinone or semiquinone moieties
561 of organic matter, as proposed by Steinberg et al. (2008a). Allard and Gallard (2013) also
562 proposed also a mechanism of abiotic formation of iodomethane from pyruvate, an organic
563 compound derived from the oxidation of humic substances. Thus, differences in the nature of
564 the humus OM according to forms of humus may also affect ^{125}I volatilization. Furthermore, it
565 has been shown that the iodine volatilization process is stimulated by biological activity in the
566 soil, by external enzymes excreted by microorganisms and/or by a wide variety of bacteria
567 (Allard et al., 2010; Amachi, 2008; Muramatsu et al., 2004; Muramatsu and Yoshida, 1995).
568 Amachi et al. (2003) showed that soil bacteria are able to methylate iodine (producting CH_3I).
569 Ban-nai et al. (2006), using laboratory cultures, found that filamentous fungi in soils
570 accumulated and volatilized ^{125}I (to 3.4% of total I in soil) in CH_3I form. Shimamoto et al.
571 (2011) and Seki et al. (2013) proposed that oxidase laccase enzyme, produced by soil fungi and
572 bacteria, is able to oxidize I^- into I_2. Although these authors suggest that I_2 reacts with OM to
573 produce organo-iodinated compounds retained in soil, it is likely that part of I_2 is directly
574 volatilized and that some organo-iodinated compounds are converted to CH_3I and then
575 volatilized. In our study, this assumption is supported by the community-level physiological
576 profiles (Figure 2) of moders (i.e. CHS35, HET29 and SP63), which decreased more slowly
577 over time than those of mulls (i.e. CHP40, HET25 and SP25), retaining positive C-sources
578 >50% up to t-56, that may maintain a higher volatilization rate throughout our experiment than
579 for mull humus.

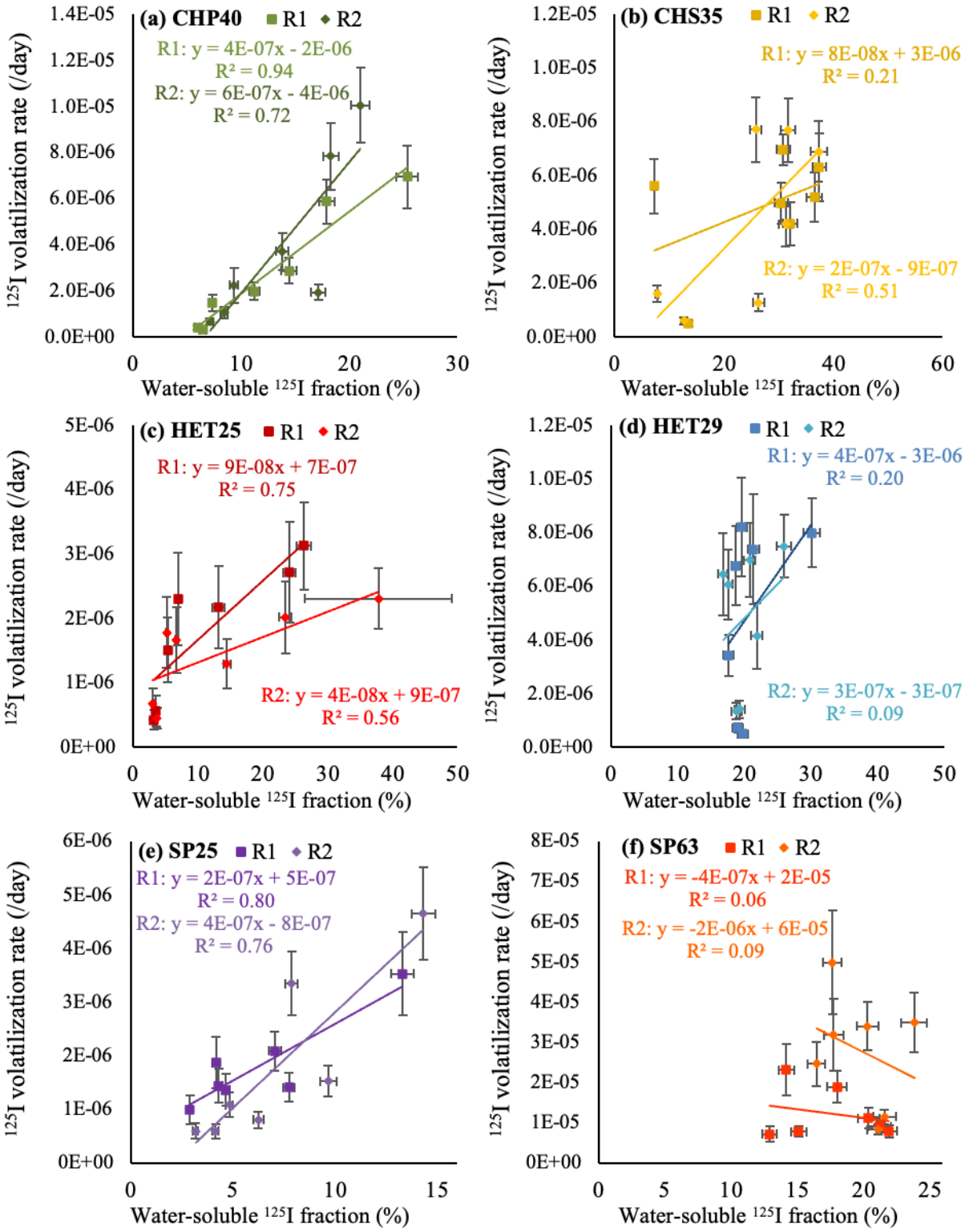

Figure 7. Mean (± standard error) of ^{125}I volatilization rate by sampling time as a function of w-soluble ^{125}I fraction according to humus sample. For these graphs, values of ^{125}I volatilized fraction correspond to mean of ^{125}I volatilization rates at some days before and after sampling time for w-soluble extraction.

Conclusion

587 Our results show that humus is a zone of iodine accumulation by association with the
588 solid phase. The w-soluble ^{125}I fraction decreased over time from ~14-37% to 3-19% depending
589 on the type of humus. As the organic iodine fraction remained stable (~38-56%), an increase in
590 residual ^{125}I was observed (from ~18-34% to 38-43). After 4 months, the proportions of w-
591 soluble, organic and residual added ^{125}I were relatively similar to results obtained for natural
592 ^{127}I, implying that added ^{125}I tended towards native iodine distribution after a few months. The
593 more complex nature of organic material in moders (slow degradation) than in mulls (fast
594 degradation) resulted in slower iodination of organic molecules and thus higher proportions of
595 w-soluble ^{125}I for moders than mulls. Significant positive correlations between ^{125}I
596 concentrations and concentrations of dissolved organic carbon in the w-soluble fraction may
597 indicate that organic matter plays a dual role, acting both as iodine sink, probably through the
598 migration of humic substances of high molecular weight, and also as source of subsurface
599 iodine dispersion, probably through humic substances of low molecular weight. This study
600 confirms that ^{125}I losses by volatilization are relatively low (total volatilized ^{125}I fractions =
601 0.01-0.47%). Although of the same order of magnitude, total ^{125}I volatilization was higher for
602 moders (~0.039-0.323%) than for mulls (~0.015-0.023%) for which volatilization rates were
603 positively correlated to w-soluble iodine fractions during incubation.
604
605 **Acknowledgments**
606 The authors would like to acknowledge the technical staff of RENECOFOR – ONF
607 (Caroline BRUYERE, Geoffroy PERALS, Mauryne VINCENT, Henri JUIF, Didier
608 LAGREDE and Yves LE VALLEGANT) for logistical support for the sampling of selected
609 humus. We would like to acknowledge Anne-Cécile GREGOIRE (IRSN/PSN-
610 RES/SEREX/L2EC) for advices and part of incubation material. This work was financed by the
611 Agence Nationale de la Recherche with funds allocated in the 'Investissements d'Avenir'

framework program under reference ANR11-RSNR-0002 and the Région Nouvelle Aquitaine. We would like to acknowledge the translation company CAUPENNE & CO for English language assistance.

Supplementary information

A map of the localisation of the six sampling sites. Figures of evolution of (i) the water contents, (ii) the fluorescence index measured in water-extracts and TMAH-extracts, (iii) the total ^{125}I activity, and (iv) the ^{125}I volatilization rates from spiked humus during incubation time. A table with the characteristics of the carbon substrates in Biolog EcoPlate™ and chemical guilds. Tables of the detailed dataset of humus parameters (i.e. pH, C content, C/N ratio, DOC concentrations) and ^{127}I and ^{129}I proportions in water- and TMAH-extracts. Tables of the modelling results of the evolutions of ^{125}I w-soluble, organic and residual fractions, and of the ^{125}I volatilization rates and cumulative fluxes.

References

Allard, S., Gallard, H., 2013. Abiotic formation of methyl iodide on synthetic birnessite: A mechanistic study. Sci. Total Environ. 463–464, 169–175. https://doi.org/10.1016/j.scitotenv.2013.05.079

Allard, S., Gallard, H., Fontaine, C., Croué, J.-P., 2010. Formation of methyl iodide on a natural manganese oxide. Water Res. 44, 4623–4629. https://doi.org/10.1016/j.watres.2010.06.008

Amachi, S., 2008. Microbial Contribution to Global Iodine Cycling: Volatilization, Accumulation, Reduction, Oxidation, and Sorption of Iodine. Microbes Environ. 23, 269–276. https://doi.org/10.1264/jsme2.ME08548

Amachi, S., Kasahara, M., Hanada, S., Kamagata, Y., Shinoyama, H., Fujii, T., Muramatsu, Y., 2003. Microbial Participation in Iodine Volatilization from Soils. Environ. Sci. Technol. 37, 3885–3890. https://doi.org/10.1021/es0210751

Ashworth, D.J., Shaw, G., Butler, A.P., Ciciani, L., 2003. Soil transport and plant uptake of radio-iodine from near-surface groundwater. J. Environ. Radioact., International workshop on the mobility of iodine, technetium, selenium and uranium in the biosphere 70, 99–114. https://doi.org/10.1016/S0265-931X(03)00121-8

Baize, D., Girard, M.C., Beaudou, A.G., Poss, R., 2009. Référentiel pédologique 2008. Quae, 405 p. (Savoir Faire). ISBN 978-2-7592-0185-3 ISSN 1952-1251

Ban-nai, T., Muramatsu, Y., Amachi, S., 2006. Rate of iodine volatilization and accumulation by filamentous fungi through laboratory cultures. Chemosphere 65, 2216–2222. https://doi.org/10.1016/j.chemosphere.2006.05.047

Bostock, A.C., Shaw, G., Bell, J.N.B., 2003. The volatilisation and sorption of ^{129}I in coniferous forest, grassland and frozen soils. J. Environ. Radioact., International workshop on the mobility of iodine, technetium, selenium and uranium in the biosphere 70, 29–42. https://doi.org/10.1016/S0265-931X(03)00120-6

Bowley, H.E., Young, S.D., Ander, E.L., Crout, N.M.J., Watts, M.J., Bailey, E.H., 2016. Iodine binding to humic acid. Chemosphere 157, 208–214. https://doi.org/10.1016/j.chemosphere.2016.05.028

Brêthes, A., Ulrich, E., 1997. RENECOFOR. Caractéristiques pédologiques des 102 peuplements du réseau, observations de 1994/95, in : Office Nationale des Forêts, Département des Recherches Techniques (Eds.), ISBN 2 - 84207 - 112 - 3, 573 p.

Carter, H.T., Tipping, E., Koprivnjak, J.-F., Miller, M.P., Cookson, B., Hamilton-Taylor, J., 2012. Freshwater DOM quantity and quality from a two-component model of UV absorbance. Water Res. 46, 4532–4542. https://doi.org/10.1016/j.watres.2012.05.021

Chang, H., Xu, C., Schwehr, K.A., Zhang, S., Kaplan, D.I., Seaman, J.C., Yeager, C., Santschi, P.H., 2014. Model of radioiodine speciation and partitioning in organic-rich and organic-poor soils from the Savannah River Site. Journal of Environmental Chemical Engineering 2, 1321–1330. https://doi.org/10.1016/j.jece.2014.03.009

Choi, K.-H., Dobbs, F.C., 1999. Comparison of two kinds of Biolog microplates (GN and ECO) in their ability to distinguish among aquatic microbial communities. J. Microbiol. Methods 36, 203–213. https://doi.org/10.1016/S0167-7012(99)00034-2

Colinon-Dupuich, C., Février, L., Ranjard, L., Coppin, F., Cournoyer, B., Nazaret, S., 2011. Radioecological Risk Assessment of Low Selenium Concentrations through Genetic Fingerprints and Metabolic Profiling of Soil Bacterial Communities. Microbial Ecology 62, 14–24. https://doi.org/10.1007/s00248-011-9831-x

Cotrufo, M.F., Ngao, J., Marzaioli, F., Piermatteo, D., 2010. Inter-comparison of methods for quantifying above-ground leaf litter decomposition rates. Plant Soil 334, 365–376. https://doi.org/10.1007/s11104-010-0388-0

675 Dai, J.L., Zhang, M., Zhu, Y.G., 2004. Adsorption and desorption of iodine by various Chinese
676 soils: I. Iodate. Environ. Int. 30, 525–530. https://doi.org/10.1016 /j.envint.2003.10.007
677 Dai, J.L., Zhang, M., Hu, Q.H., Huang, Y.Z., Wang, R.Q., Zhu, Y.G., 2009. Adsorption and
678 desorption of iodine by various Chinese soils: II. Iodide and iodate. Geoderma 153,
679 130–135. https://doi.org/10.1016/j.geoderma.2009.07.020
680 Duchaufour, P., 1950. L'humus forestier et les facteurs de sa décomposition, in : Revue
681 forestière française (Eds). https://doi.org/10.4267/2042/27708
682 Franke, K., Kupsch, H., 2010. Radioiodination of humic substances. Radiochim. Acta 98, 333–
683 339. https://doi.org/10.1524/ract.2010.1721
684 Fukui, M., Fujikawa, Y., Satta, N., 1996. Factors affecting interaction of radioiodide and iodate
685 species with soil. J. Environ. Radioact. 31, 199–216. https://doi.org/10.1016/0265-
686 931X(95)00039-D
687 Glimm, E., Heuer, H., Engelen, B., Smalla, K., Backhaus, H., 1997. Statistical comparisons of
688 community catabolic profiles. J. Microbiol. Methods 30, 71–80.
689 https://doi.org/10.1016/S0167-7012(97)00046-8
690 Grove, J.., Kautola, H., Javadpour, S., Moo-Young, M., Anderson, W.., 2004. Assessment of
691 changes in the microorganism community in a biofilter. Biochem. Eng. J. 18, 111–114.
692 https://doi.org/10.1016/S1369-703X(03)00182-7
693 Hansen, V., Roos, P., Aldahan, A., Hou, X., Possnert, G., 2011. Partition of iodine (^{129}I and
694 ^{127}I) isotopes in soils and marine sediments. J. Environ. Radioact. 102, 1096–1104.
695 https://doi.org/10.1016/j.jenvrad.2011.07.005
696 Hou, X., Hansen, V., Aldahan, A., Possnert, G., Lind, O.C., Lujaniene, G., 2009. A review on
697 speciation of iodine-129 in the environmental and biological samples. Anal. Chim. Acta
698 632, 181–196. https://doi.org/10.1016/j.aca.2008.11.013
699 Hou, X.L., Fogh, C.L., Kucera, J., Andersson, K.G., Dahlgaard, H., Nielsen, S.P., 2003. Iodine-
700 129 and Caesium-137 in Chernobyl contaminated soil and their chemical fractionation.
701 Sci. Total Environ. 308, 97–109. https://doi.org/10.1016/S0048-9697(02)00546-6
702 Johnson, C.C., 1980. The Geochemistry of Iodine and a Preliminary Investigation into its
703 Potential Use as a Pathfinder Element in Geochemical Exploration. PhD Thesis.
704 University College of Wales, Aberystwyth.
705 Johnson, M.S., Couto, E.G., Abdo, M., Lehmann, J., 2011. Fluorescence index as an indicator
706 of dissolved organic carbon quality in hydrologic flowpaths of forested tropical
707 watersheds. Biogeochemistry 105, 149–157. https://doi.org/10.1007/s10533-011-9595-
708 x
709 Keppler, F., Borchers, R., Elsner, P., Fahimi, I., Pracht, J., Schöler, H.F., 2003. Formation of
710 volatile iodinated alkanes in soil: results from laboratory studies. Chemosphere,
711 Naturally Produced Organohalogens 52, 477–483. https://doi.org/10.1016/S0045-
712 6535(03)00198-X
713 Leflaive, J., Céréghino, R., Danger, M., Lacroix, G., Ten-Hage, L., 2005. Assessment of self-
714 organizing maps to analyze sole-carbon source utilization profiles. J. Microbiol.
715 Methods 62, 89–102. https://doi.org/10.1016/j.mimet.2005.02.002
716 McKnight, D.M., Boyer, E.W., Westerhoff, P.K., Doran, P.T., Kulbe, T., Andersen, D.T., 2001.
717 Spectrofluorometric characterization of dissolved organic matter for indication of
718 precursor organic material and aromaticity. Limnology and Oceanography 46, 38–48.
719 https://doi.org/10.4319/lo.2001.46.1.0038
720 Mercier, F., Moulin, V., Guittet, M.J., Barre, N., Toulhoat, N., Gautier-Soyer, M., Toulhoat, P.,
721 2000. Applications of NAA, PIXE and XPS for the Quantification and Characterization
722 of the Humic Substances/Iodine Association. Radiochim. Acta 88, 779–785.
723 https://doi.org/10.1524/ract.2000.88.9-11.779

724 Muramatsu, Y., Uchida, S., Sriyotha, P., Sriyotha, K., 1990. Some considerations on the
725 sorption and desorption phenomena of iodide and iodate on soil. Water Air Soil Pollut.
726 49, 125–138. https://doi.org/10.1007/BF00279516
727 Muramatsu, Y., Yoshida, S., 1995. Volatilization of methyl iodide from the soil-plant system.
728 Atmos. Environ. 29, 21–25. https://doi.org/10.1016/1352-2310(94)00220-F
729 Muramatsu, Y., Yoshida, S., Fehn, U., Amachi, S., Ohmomo, Y., 2004. Studies with natural
730 and anthropogenic iodine isotopes: iodine distribution and cycling in the global
731 environment. J. Environ. Radioact. 74, 221–232.
732 https://doi.org/10.1016/j.jenvrad.2004.01.011
733 Pietikäinen, J., Pettersson, M., Bååth, E., 2005. Comparison of temperature effects on soil
734 respiration and bacterial and fungal growth rates. FEMS Microbiol. Ecol. 52, 49–58.
735 https://doi.org/10.1016/j.femsec.2004.10.002
736 Pohlad, B., Owen, B., 2009. Biolog Ecoplate Standard Methods. Ferrum College Watershed
737 Studies. TAS Technical Bulletin.
738 Qiao, J., Hansen, V., Hou, X., Aldahan, A., Possnert, G., 2012. Speciation analysis of ^{129}I, ^{137}Cs,
739 ^{232}Th, ^{238}U, ^{239}Pu and ^{240}Pu in environmental soil and sediment. Appl. Radiat. Isot. 70,
740 1698–1708. https://doi.org/10.1016/j.apradiso.2012.04.006
741 Ranger, J., Colin-Belgrand, M., Nys, C., 1995. Le cycle biogéochimique des éléments majeurs
742 dans les écosystèmes forestiers. Importance dans le fonctionnement des sols.
743 Reiller, P., Mercier-Bion, F., Gimenez, N., Barre, N., Miserque, F., 2006. Iodination of Humic
744 Acid Samples from Different Origins. Radiochim. Acta 94, 739–745.
745 https://doi.org/10.1524/ract.2006.94.9-11.739
746 Roulier, M., Bueno, M., Thiry, Y., Coppin, F., Redon, P.-O., Le Hécho, I., Pannier, F., 2018.
747 Iodine distribution and cycling in a beech (*Fagus sylvatica*) temperate forest. Sci. Total
748 Environ. 645, 431–440. https://doi.org/10.1016/j.scitotenv.2018.07.039
749 Roulier, M., Coppin, F., Bueno, M., Nicolas, M., Thiry, Y., Della Vedova, C., Février, L.,
750 Pannier, F., Le Hécho, I., 2019. Iodine budget in forest soils: Influence of environmental
751 conditions and soil physicochemical properties. Chemosphere 224, 20–28.
752 https://doi.org/10.1016/j.chemosphere.2019.02.060
753 Santschi, P.H., Xu, C., Zhang, S., Schwehr, K.A., Grandbois, R., Kaplan, D.I., Yeager, C.M.,
754 2017. Iodine and plutonium association with natural organic matter: A review of recent
755 advances. Appl. Geochem., Transformation and Fate of Natural and Anthropogenic
756 Radionuclides in the Environments 85, 121–127.
757 https://doi.org/10.1016/j.apgeochem.2016.11.009
758 Schlegel, M.L., Reiller, P., Mercier-Bion, F., Barré, N., Moulin, V., 2006. Molecular
759 environment of iodine in naturally iodinated humic substances: Insight from X-ray
760 absorption spectroscopy. Geochim. Cosmochim. Acta 70, 5536–5551.
761 https://doi.org/10.1016/J.GCA.2006.08.026
762 Schwehr, K.A., Santschi, P.H., Kaplan, D.I., Yeager, C.M., Brinkmeyer, R., 2009. Organo-
763 Iodine Formation in Soils and Aquifer Sediments at Ambient Concentrations. Environ.
764 Sci. Technol. 43, 7258–7264. https://doi.org/10.1021/es900795k
765 Seki, M., Oikawa, J., Taguchi, T., Ohnuki, T., Muramatsu, Y., Sakamoto, K., Amachi, S., 2013.
766 Laccase-Catalyzed Oxidation of Iodide and Formation of Organically Bound Iodine in
767 Soils. Environ. Sci. Technol. 47, 390–397. https://doi.org/10.1021/es303228n
768 Shaw, G., 2007. Radionuclides in forest ecosystems, in: Radioactivity in the Environment.
769 Elsevier, pp. 127–155.
770 Sheppard, M.I., Thibault, D.H., Smith, P.A., Hawkins, J.L., 1994. Volatilization: a soil
771 degassing coefficient for iodine. J. Environ. Radioact. 25, 189–203.
772 https://doi.org/10.1016/0265-931X(94)90072-8

Shetaya, W.H., Young, S.D., Watts, M.J., Ander, E.L., Bailey, E.H., 2012. Iodine dynamics in soils. Geochim. Cosmochim. Acta 77, 457–473. https://doi.org/10.1016/j.gca.2011.10.034

Shimamoto, Y.S., Takahashi, Y., Terada, Y., 2011. Formation of Organic Iodine Supplied as Iodide in a Soil−Water System in Chiba, Japan. Environ. Sci. Technol. 45, 2086–2092. https://doi.org/10.1021/es1032162

Sive, B.C., Varner, R.K., Mao, H., Blake, D.R., Wingenter, O.W., Talbot, R., 2007. A large terrestrial source of methyl iodide. Geophys. Res. Lett. 34, L17808. https://doi.org/10.1029/2007GL030528

Söderlund, M., Virkanen, J., Aromaa, H., Gracheva, N., Lehto, J., 2017. Sorption and Speciation of Iodine in Boreal Forest Soil. J. Radioanal. Nucl. Chem. 311, 549–64. https://doi.org/10.1007/s10967-016-5022-z.

Steinberg, S.M., Kimble, G.M., Schmett, G.T., Emerson, D.W., Turner, M.F., Rudin, M., 2008a. Abiotic reaction of iodate with sphagnum peat and other natural organic matter. J. Radioanal. Nucl. Chem. 277, 185–191. https://doi.org/10.1007/s10967-008-0728-1

Steinberg, S.M., Schmett, G.T., Kimble, G., Emerson, D.W., Turner, M.F., Rudin, M., 2008b. Immobilization of fission iodine by reaction with insoluble natural organic matter. J. Radioanal. Nucl. Chem. 277, 175–183. https://doi.org/10.1007/s10967-008-0727-2

Takeda, A., Tsukada, H., Takahashi, M., Takaku, Y., Hisamatsu, S., 2015. Changes in the chemical form of exogenous iodine in forest soils and their extracts. Radiat. Prot. Dosimetry 167, 181–186. https://doi.org/10.1093/rpd/ncv240

Takeda, A., Unno, Y., Tsukada, H., Takaku, Y., Hisamatsu, S., 2019. Speciation of iodine in soil solution in forest and grassland soils in rokkasho, Japan. Radiat. Prot. Dosimetry 184, 368–371. https://doi.org/10.1093/rpd/ncz103

Teramage, M.T., Carasco, L., Orjollet, D., Coppin, F., 2018. The impact of radiocesium input forms on its extractability in Fukushima forest soils. J. Hazard. Mater. 349, 205–214. https://doi.org/10.1016/j.jhazmat.2018.01.047

Unno, Y., Tsukada, H., Takeda, A., Takaku, Y., Hisamatsu, S., 2017. Soil-soil solution distribution coefficient of soil organic matter is a key factor for that of radioiodide in surface and subsurface soils. J. Environ. Radioact. 169–170, 131–136. https://doi.org/10.1016/j.jenvrad.2017.01.016

UNSCEAR, 2011. Sources and effects of ionizing radiation: UNSCEAR 2008 report to the General Assembly, with scientific indexes Vol. 2, United Nations, New York.

Verschuere, L., Fievez, V., Vooren, L., Verstraete, W., 1997. The contribution of individual populations to the Biolog pattern of model microbial communities. FEMS Microbiol. Ecol. 24, 353–362. https://doi.org/10.1111/j.1574-6941.1997.tb00452.x

Warner, J.A., Casey, W.H., Dahlgren, R.A., 2000. Interaction Kinetics of I_2 (aq) with substituted phenols and humic substances. Environ. Sci. Technol. 34, 3180–3185. https://doi.org/10.1021/es991228t

Watts, M.J., Mitchell, C.J., 2008. A pilot study on iodine in soils of Greater Kabul and Nangarhar provinces of Afghanistan. Environ. Geochem. Health 31, 503–509. https://doi.org/10.1007/s10653-008-9202-9

Whitehead, D.C., 1973. Studies on Iodine in British Soils. J. Soil Sci. 24, 260–270. https://doi.org/10.1111/j.1365-2389.1973.tb00763.x

Whitehead, D.C., 1978. Iodine in Soil Profiles in Relation to Iron and Aluminium Oxides and Organic Matter. J. Soil Sci. 29, 88–94. https://doi.org/10.1111/j.1365-2389.1978.tb02035.x

Wildung, R.E., Cataldo, D.A., Garland, T.R., 1985. Volatilization of iodine from soils and plants. Speciation of Fission and Activation Products in the Environment. 243–9.

Xu, C., Miller, E.J., Zhang, S., Li, H.-P., Ho, Y.-F., Schwehr, K.A., Kaplan, D.I., Otosaka, S., Roberts, K.A., Brinkmeyer, R., Yeager, C.M., Santschi, P.H., 2011a. Sequestration and Remobilization of Radioiodine (^{129}I) by Soil Organic Matter and Possible Consequences of the Remedial Action at Savannah River Site. Environ. Sci. Technol. 45, 9975–9983. https://doi.org/10.1021/es201343d

Xu, C., Zhang, S., Ho, Y.-F., Miller, E.J., Roberts, K.A., Li, H.-P., Schwehr, K.A., Otosaka, S., Kaplan, D.I., Brinkmeyer, R., Yeager, C.M., Santschi, P.H., 2011b. Is soil natural organic matter a sink or source for mobile radioiodine (^{129}I) at the Savannah River Site? Geochim. Cosmochim. Acta 75, 5716–5735. https://doi.org/10.1016/j.gca.2011.07.011

Xu, C., Zhong, J., Hatcher, P.G., Zhang, S., Li, H.-P., Ho, Y.-F., Schwehr, K.A., Kaplan, D.I., Roberts, K.A., Brinkmeyer, R., Yeager, C.M., Santschi, P.H., 2012. Molecular environment of stable iodine and radioiodine (^{129}I) in natural organic matter: Evidence inferred from NMR and binding experiments at environmentally relevant concentrations. Geochim. Cosmochim. Acta 97, 166–182. https://doi.org/10.1016/j.gca.2012.08.030

Xu, C., Chen, H., Sugiyama, Y., Zhang, S., Li, H.P., Ho, Y.F., Chuang, C.Y., Schwehr, K.A., Kaplan, D.I., Yeager, C., Roberts, K.A., Hatcher, P.G., Santschi, P.H. 2013. Novel Molecular-Level Evidence of Iodine Binding to Natural Organic Matter from Fourier Transform Ion Cyclotron Resonance Mass Spectrometry. Sci. Total Environ. 449, 244–252. https://doi.org/10.1016/j.scitotenv.2013.01.064